PAPER

Interaction of silicene with amino acid analogues—from physical to chemical adsorption in gas and solvated phases

View the article online for updates and enhancements.

2D Materials

Interaction of silicene with amino acid analogues—from physical to chemical adsorption in gas and solvated phases

Yesukhei Jagvaral[1], Haiying He[1] and Ravindra Pandey[2]

1   Department of Physics and Astronomy, Valparaiso University, Valparaiso, IN 46383 United States of America
2   Department of Physics, Michigan Technological University, Houghton, MI 49931, United States of America

E-mail: haiying.he@valpo.edu and pandey@mtu.edu

Abstract

Silicene is an emerging 2D material, and an understanding of its interaction with amino acids, the basic building blocks of protein, is of fundamental importance. In this paper, we investigate the nature of adsorption of amino-acid analogues on silicene employing density functional theory and an implicit solvation model. Amino acid analogues are defined as CH_3–R molecules, where R is the functional group of the amino acid side chain. The calculated results find three distinct groups within the amino-acid analogues considered: (i) group I, which includes $MeCH_3$ and $MeSH$, interacts with silicene via the van der Waals dispersive terms leading to physisorbed configurations; (ii) group II strongly interacts with silicene forming Si–O/N chemical bonds in the chemisorbed configurations; and (iii) group III, which consists of the phenyl group, interacts with silicene via π–π interactions leading to physisorbed configurations. The results show that the lateral chains of the amino acids intrinsically determine the interactions between protein and silicene at the interface under the given physiological conditions.

1. Introduction

Silicene is one of the emerging nanomaterials that is very similar to graphene in its honeycomb-type of structure and electronic properties, except for buckling. The buckled structure of silicene is due to the preference of Si atoms to adopt both sp^3 and sp^2 hybridization rather than adopting sp^2 hybridization alone, as in graphene [1]. As a result, silicene shows a higher degree of chemical reactivity to atoms [2–7] and molecules [8–12], and has been proposed as a promising chem/bio sensing material. For example, Amorim and Scheicher, investigating the interaction of silicene with purine and pyrimidine nucleobases, suggested that silicene could be utilized as an integrated-circuit biosensor as part of a lab-on-a-chip device for DNA analysis [13]. In addition, recent theoretical studies based on density functional theory (DFT) have shown that silicene could be used for highly sensitive molecule and gas sensors [9, 10]. Furthermore, silicene exhibits some unique physical properties such as the spin Hall effect, semi-metallicity, tunability of the band gap, and modulation of the reflectivity with doping, as summarized in a

recent review [14]. Silicene, as a natural derivative of Si, demonstrates better compatibility and easier integration with existing Si nanotechnology for novel applications, and it has been synthesized on a variety of substrates, such as Ag [1, 15–17], Ir [18], ZrB_2 [19] and ZrC [20].

In porous silicon, a recent protein adsorption kinetics study demonstrated the feasibility of its label-free detection of protein adsorption in real time [21]. On the other hand, using a combined experimental and computational approach, Rahsepar *et al* proposed the adsorption and film growth mechanisms of proteinogenic biomolecules on a Si(1 1 1) 7×7 surface and pointed out the particular role of hydrogen bonding interactions of biological molecules in such systems [22]. As the basic building blocks of protein, a fundamental understanding of the interaction of amino acids with silicene is therefore required, as this would provide atomic-level insight into the protein–silicene interface. This fact is further reaffirmed by recent single-molecule force spectroscopy measurements of amino acid residues, such as lysine, glutamate, phenylalanine, leucine, and glutamine, which revealed a distinguishably different strength of

interaction between the individual amino acid residues and the silicon substrate [23]. In addition, adsorption of the residues on the substrate has shown to be modified with the pH and ionic strength of the solution [23].

Previously reported DFT investigations involving proteins with 2D materials have been mostly limited to a few amino acids (or analogues). In gas phase, Rimola studied interactions between several amino acid analogues (AAs) and boron-nitride (BN) nanomaterials, and reported significant differences among BN nanotubes (BNNTs) and BN monolayers (BNMLs) in the nature of the adsorption in the gas phase [24]. Based on the side groups, intrinsic affinity scales of the considered AAs for BN nanomaterials have been proposed [24]. In solvent, Waters *et al* established the relationship between the topology of BN nanomaterials and the protonated/deprotonated states of AAs [25].

In this paper, interaction of silicene with the canonical (standard) AAs will be investigated employing the DFT with inclusion of the van der Waals (vdW) interaction terms. AAs are molecules of the form CH_3-R (or MeR), where R represents the functional groups present in the side chains. The backbone is simulated by the methyl group. The amino acid residues considered are with R being CH_3, SH, OH, COOH, $CONH_2$, NH_2, imidazole, guanidine, phenyl, phenol, indole, and $CONHCH_3$, representing the seven classes of natural amino acids: aliphatic, sulfur-containing, hydroxylic, acidic, basic, aromatic, and amidic, as listed in table 1. Since the lateral chains of the amino acids are more likely to interact with silicene, the results will provide insights featuring which amino acids are likely to dominate the protein–silicene interaction at the atomic level. The binding features of the conjugated systems will be discussed in terms of geometries, energies, charge transfers, molecular orbitals and polarizabilities. Considering that most of the biological and physiological processes occur in solvent, we will perform calculations in both the gas and solvated phases. The effect of solvent will be further explored by investigating the zwitterion form of some of the AAs in solvent.

2. Computational method

Electronic structure calculations based on the DFT were performed with the B3LYP functional form [26, 27] together with the 6-31G(d,p) basis sets using the program package Gaussian 09 [28]. Contributions from vdW dispersion forces were included in the form of the Grimme-D2 terms in the calculations [29]. The polarizable continuum model [30] was used to mimic the solvent effect, which computes the energy in solution by making the solvent reaction field self-consistent with the solute electrostatic potential generated from the computed electron density. For water, a dielectric constant $\varepsilon = 78.35$ was used.

Comparison to other solvation models and dispersion corrections is provided in the supplementary information table S1 (stacks.iop.org/TDM/5/015012/mmedia) and the results are fairly consistent. The charge analysis of a conjugated configuration was performed using the natural bond orbital (NBO) analysis [31].

A cluster model approach was adopted to simulate silicene, where the sheet is modeled by a finite Si_{48} cluster consisting of a central hexagon and two neighboring bands of rings to minimize effectively edge effects. In addition, the Si edge atoms were passivated by hydrogen atoms making the cluster $Si_{48}H_{18}$. A larger model of silicene, $Si_{96}H_{24}$ was tested and this resulted in very comparable results (see supplementary information figure S1 for the models and comparison of results thereafter). This approach has been successfully employed for a long time in using accurate *ab initio* methods of quantum chemistry for a quantitative description and detailed understanding of the interaction between atoms and molecules and a solid surface. An early example [32] is the study of the adsorption and surface penetration of atomic hydrogen at the open site of Si(111), which resembles the hydrogen/silicene system. Recent examples include stability and electronic properties of pyrazinamide conjugated silicene [33] and proton and hydrogen transport through silicene [34].

Following the nomenclature of AAs [24], twelve AAs were considered (table 1), including MeCH$_3$ and MeSH as analogues of alanine and cysteine, respectively. Alanine is a simple amino acid and its side chain $-R$ is $-CH_3$. To determine the equilibrium configurations of the conjugated complexes, molecules were initially placed on silicene at different lattice sites (e.g. atop, bridge and hole/center) with different orientations, including the parallel and perpendicular orientations relative to the surface. Then, the geometry optimization calculations without applying symmetry constraints were performed. The convergence criteria in maximum force, RMS force, maximum displacement, and RMS displacement were set as $0.023\,\text{eV}\,\text{Å}^{-1}$, $0.015\,\text{eV}\,\text{Å}^{-1}$, $9.5 \times 10^{-4}\,\text{Å}$, $6.4 \times 10^{-4}\,\text{Å}$, respectively. Note that the equilibrium configuration of the pristine silicene was buckled with an out-of-plane vertical distance of $\sim 0.44\,\text{Å}$ (for outer edges) and $0.40\,\text{Å}$ (for central Si atoms), which is in agreement with the previous report of $0.44\,\text{Å}$ obtained using a model with periodic boundary conditions [35].

The binding energy, E_b of the AAs with silicene was computed as:

$$E_b = (E_{\text{molecule}} + E_{\text{silicene}}) - E_{\text{molecule/silicene}} \quad (1)$$

where $E_{\text{molecule/silicene}}$, E_{silicene} and E_{molecule} are the total energies of the molecule–silicene conjugate, silicene, and molecule, respectively. The positive value of E_b suggests the stability of the conjugated complex.

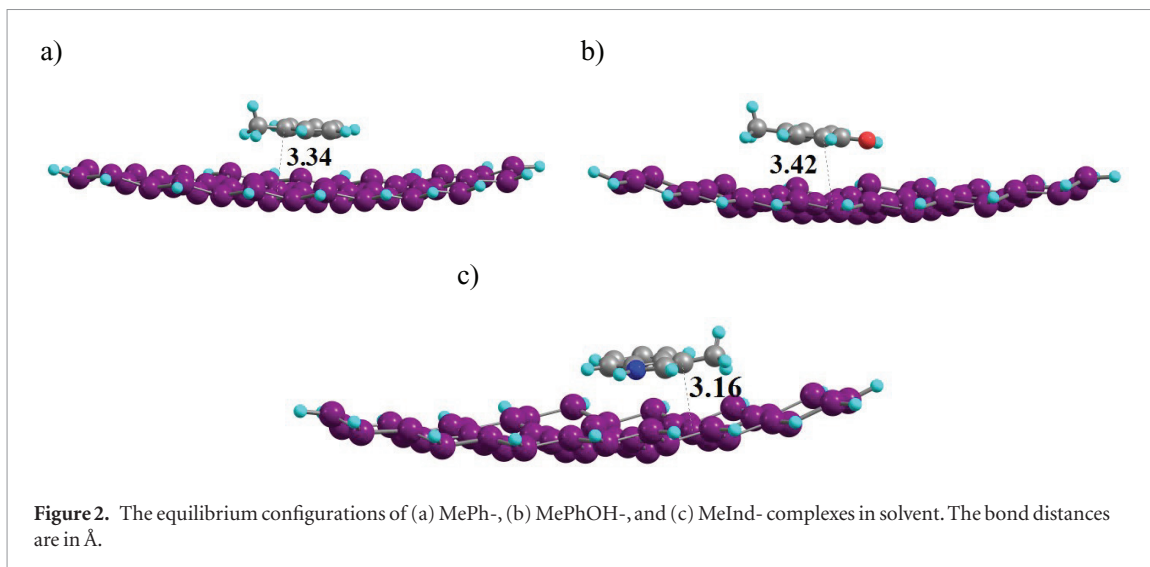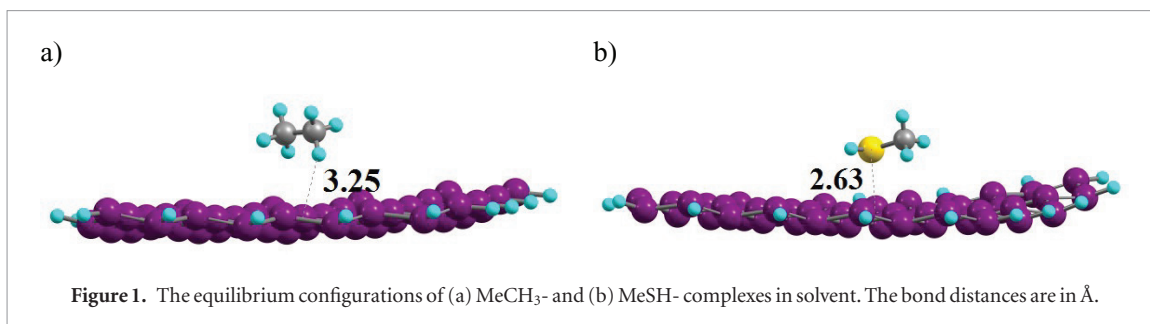**Table 1.** Amino acids and their analogues considered in this study.

No.	Amino acid (class)	AA (neutral) Name	AA (neutral) Structure
1	Alanine (aliphatic)	MeCH$_3$	
2	Cysteine (S-containing)	MeSH	
3	Aspartic acid (acidic)	MeCOOH	
4	Serine (hydroxylic)	MeOH	
5	Asparagine (amidic)	MeCONH$_2$	
6	Peptide bond	MeCONHMe	
7	Lysine (basic)	MeNH$_2$	
8	Histidine (basic)	MeIm	
9	Arginine (basic)	MeGua	
10	Phenylalanine (aromatic)	MePh	
11	Tyrosine (aromatic)	MePhOH	
12	Tryptophan (aromatic)	MeInd	

3. Results and discussion

3.1. Canonical AAs
Figures 1–3 display the calculated equilibrium configurations of the conjugated complexes in solvent, and the corresponding structural properties in both gas and solvated phases are listed in table 2. The gas-phase equilibrium configurations of the conjugated complexes are shown in figure S2 of the supplementary information.

In going from gas to solvent, the binding energies for (i) MeCONH$_2$, MeCONHMe, MeNH$_2$, MeIm, and MeGua show an increase of about 0.1–0.2 eV; MeCH$_3$, MeCOOH and MeOH show a slight increase of about ≈0.1 eV; and MeSH, MePh, MePhOH and MeInd show a slight decrease of about ≈0.1 eV. A small variation in binding energy in response to the aqueous environment suggests that the interaction at the interface is not dominated by electrostatic interactions [36]. Figure 4 displays contributions from dispersive

Figure 1. The equilibrium configurations of (a) MeCH$_3$- and (b) MeSH- complexes in solvent. The bond distances are in Å.

Figure 2. The equilibrium configurations of (a) MePh-, (b) MePhOH-, and (c) MeInd- complexes in solvent. The bond distances are in Å.

terms to the total binding energies of the complexes in solvent where the assigned numbers on the *x*-axis are taken from table 1 representing the AAs.
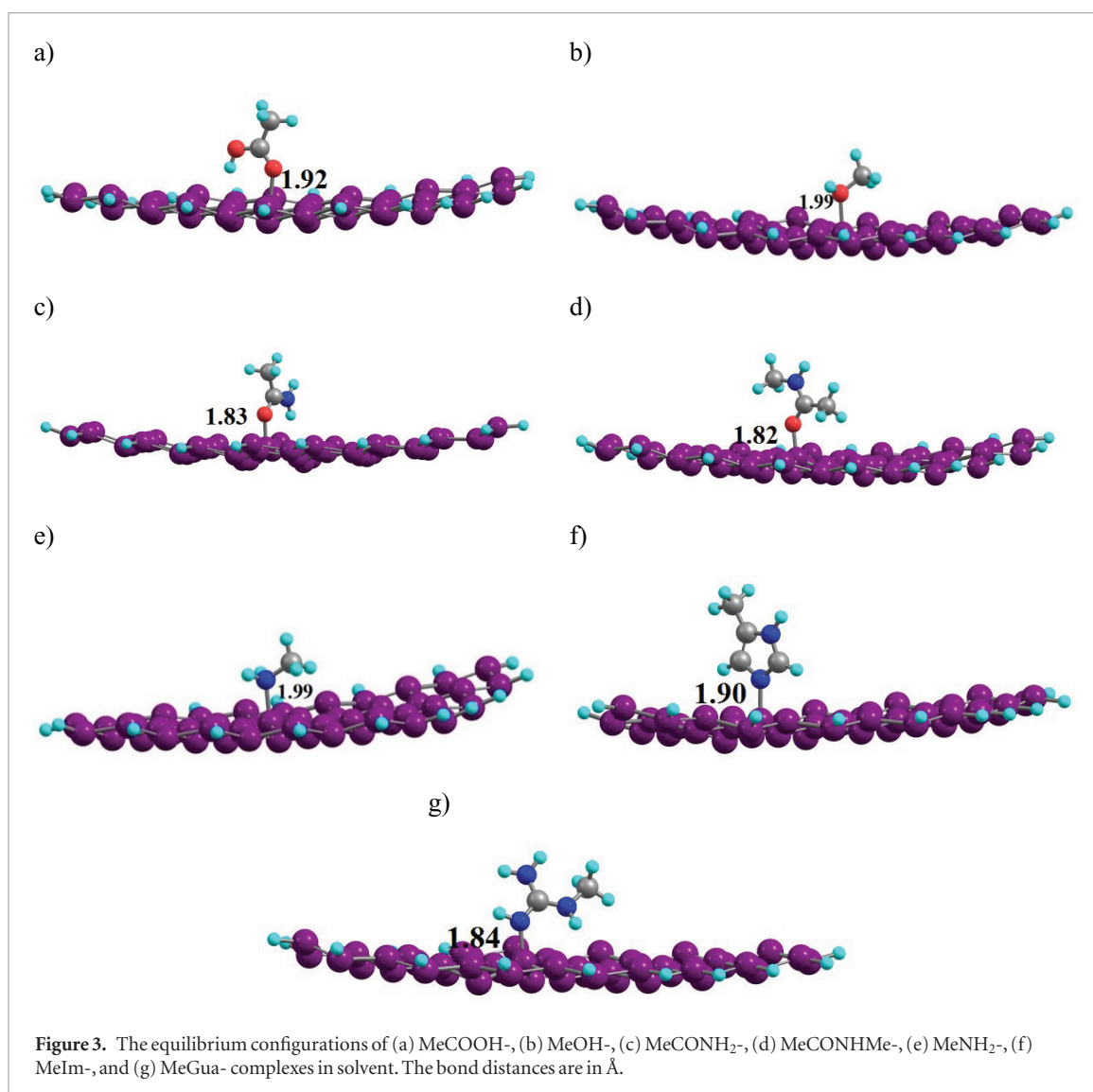
The interaction strength in terms of the binding energy for MeCH$_3$ and MeSH is rather weak (figure 1, table 2). The small attractive force comes from the vdW interaction terms (figure 4), whereas the even smaller repulsive force is likely due to the electrostatic interactions of like charges when the AAs approach silicene. The side group −CH$_3$ of MeCH$_3$ is inert and sits on the top of the surface with a nearest-neighbor distance of 3.09 Å (figure 1), with negligible charge transfer. On the other hand, the side group −SH of MeSH presents a unique case of a non-chemical bonded configuration in solvent with a relatively large charge transfer of 0.30*e* from molecule to silicene and a relatively small binding energy (table 2).

Figure 2 shows the equilibrium configurations of MePh-, MePhOH-, and MeInd-complexes where the analogues are interacting with silicene primarily through their phenyl groups. The π bonds of adducts lie at the phenyl groups of the molecules. The molecular orientations are nearly parallel to the surface, suggesting the dominance of the π–π interactions with the nearest-neighbor distances of 3.3–3.5 Å for MePh and MePhOH, and 3.2 Å for MeInd where it is also interacting via its N atom with silicene. This is further affirmed in figure 4, which displays contributions from the dispersive terms to the total binding energy, which are rather large. It is, however, interesting to note that these inter-molecular distances are comparable to,

or even smaller than, that found for benzene dimers in the slipped parallel configuration, suggesting a contribution from the electrostatic interaction as well. Among the three, MeInd shows the strongest interaction strength, and is followed by MePhOH.

Figure 3 shows the equilibrium configurations of MeCOOH, MeOH, MeCONH$_2$, MeCONHMe, MeNH$_2$, MeIm, and MeGua, which display strong interactions of molecules with silicene through O and N atoms. Here, the Si atom that is bonded with O or N 'bulges out' of the surface due to the strengthened sp^3 hybridization at the surface. The MeNH$_2$-, MeIm-, and MeGua- complexes have a relatively large binding energy with a Si–N bond distance of 1.8–2.0 Å. This is because silicene is acidic, while N-containing neutral species are basic. This fact leads to their interactions being stronger than those governed by the Si–O bonding. For example, MeCONH$_2$ and MeCONHMe are both bonded to silicene through O with a binding energy of 0.9 eV. For MeCOOH and MeOH, the binding energy is 0.35–0.45 eV. The same trend in basicity applies to the series of MeInd > MePhOH > MePh.

It is also interesting to note the differences in contributions from the dispersion forces among these analogue molecules, which can be used to classify the nature of interaction into three groups: group I representing physisorbed configurations is composed of MeCH$_3$ and MeSH, where the weak binding is driven by the vdW interactions. Group II is composed of most of the analogues (figure 4) with a relatively large binding energy due to the Si–O/N bonding in the

Figure 3. The equilibrium configurations of (a) MeCOOH-, (b) MeOH-, (c) MeCONH$_2$-, (d) MeCONHMe-, (e) MeNH$_2$-, (f) MeIm-, and (g) MeGua- complexes in solvent. The bond distances are in Å.

complexes. This yields the chemisorbed conjugated system. Group III consists of physisorbed configurations where the predominant interaction comes from the phenyl group interacting with silicene via the π–π interactions (figure 4). In addition, the relatively small intermolecular distances (3.2–3.4 Å) also suggest a contribution from electrostatic interaction due to small charge transfer. It is worth mentioning that the interaction of AAs with silicene displays a significantly different feature as compared to that with a BNML [24] and graphene [37]. In the cases of a BNML and pristine graphene, amino acids or analogues prefer dispersive interactions yielding molecules to be in parallel with the monolayer in their equilibrium configurations. There is no chemical bonding found and the binding is featured by physical adsorption.

3.2. Conjugated complexes: interaction strength and molecular properties

To understand the predicted nature of interactions in these conjugated complexes, we now examine the relationship between the calculated binding energy and the charge transfer between the molecule and silicene (figure 5). The calculated results find distinctly

Table 2. Calculated binding energy (E_b), the nearest-neighbor distance between the molecule and silicene (R_{nn}), and the charge transfer from molecule to silicene (dQ).

No.	System	Gas phase			Solvent		
		E_b (eV)	R_{nn} (Å)	dQ (e)	E_b (eV)	R_{nn} (Å)	dQ (e)
1	MeCH$_3$	0.15	3.16	0.01	0.16	3.09	0.01
2	MeSH	0.22	3.13	0.06	0.18	2.63	0.30
3	MeCOOH	0.35	1.92	0.14	0.35	1.92	0.18
4	MeOH	0.39	1.99	0.14	0.45	1.99	0.18
5	MeCONH$_2$	0.76	1.83	0.20	0.88	1.83	0.25
6	MeCON-HMe	0.71	1.82	0.20	0.89	1.82	0.25
7	MeNH$_2$	0.88	1.99	0.23	1.07	1.99	0.27
8	MeIm	1.04	1.90	0.23	1.15	1.90	0.27
9	MeGua	1.61	1.87	0.29	1.70	1.84	0.34
10	MePh	0.51	3.34	0.07	0.46	3.34	0.07
11	MePhOH	0.66	3.42	0.09	0.59	3.42	0.10
12	MeInd	0.80	3.16	0.19	0.75	3.16	0.23

different relationships for the chemisorbed and physisorbed configurations. For the chemisorbed configurations, a nearly linear relationship of the
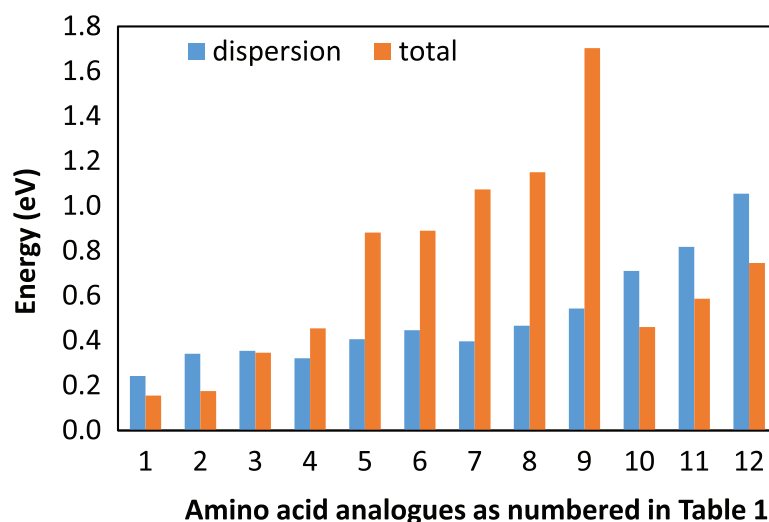
Figure 4. Calculated binding energies for the conjugated complexes where contributions from dispersive terms are given in blue. The assigned numbers on the *x*-axis are taken from table 1 representing the AAs.
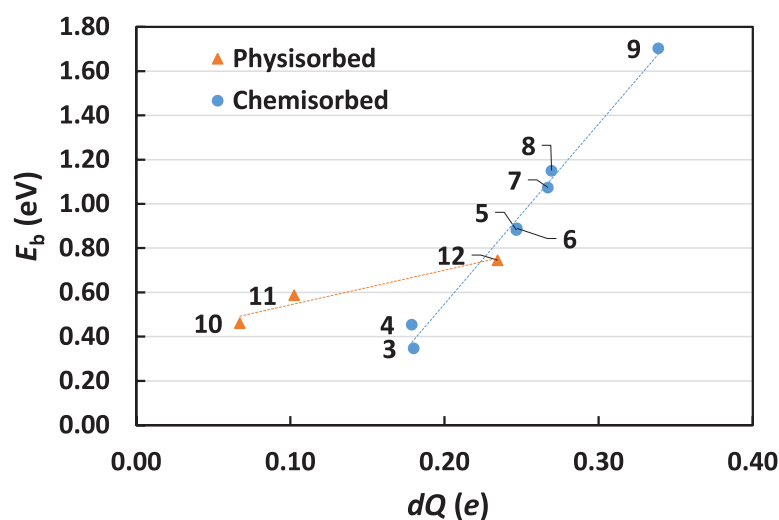

Figure 5. Conjugated complexes in solvent: binding energy versus charge transfer from molecule to silicene obtained from the NBO analysis (table 2).
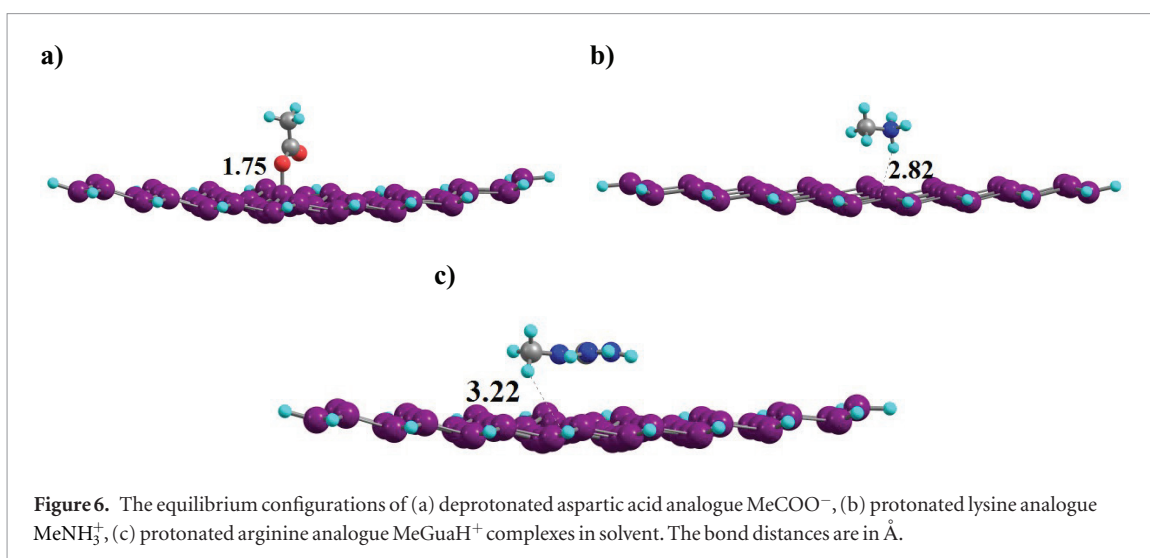
binding energy with the magnitude of the charge transfer suggests that the NBO charge may be a good indicator of the binding strength at the biomolecule–silicene interface. Furthermore, we find that the energy levels of the highest occupied molecular orbital of the AAs shows a good correlation with the degree of charge transfer from molecule to silicene in the conjugated complexes (figure S3, supplementary information).

A closer look at the analogue molecules forming chemical bonds with silicene suggests that the interaction of these molecules with silicene can be taken as a base–acid interaction. Silicene is acidic, suggesting a linear relationship between the basicity of the AA molecule and the interaction strength at the interface. For example, the carboxylic acid group ($-$COOH) has the highest acidity, thus the lowest basicity among the analogues, and the calculated binding strength of MeCOOH with silicene is the lowest (table 2). On the other hand, the presence of N increases the basicity

Table 3. Calculated binding energies (E_b) of the charged analogue complexes, and the change in binding energies (ΔE_b) as compared to the neutral species in solvent.

Charged	E_b (eV)	ΔE_b (eV)
MeCOO$^-$	2.16	1.81
MeNH$_3^+$	0.21	$-$0.86
MeGuaH$^+$	0.37	$-$1.33

of $-$CONH$_2$ or $-$CONHMe. Although the bonding is still through the O atom as in $-$COOH and $-$CONH$_2$, the interaction strength is higher in $-$CONH$_2$. The amine group ($-$NH$_2$) is a typical base. Its interaction strength with silicene rises above 1.0 eV. Likewise, the interaction strength continues to increase with the increase in the number of N atoms in the analogue molecule for the imidazole ring. The guanidine group (i.e. $-$NH$-$C(NH)NH$_2$ or $-$N $=$ C(NH$_2$)NH$_2$) has the highest basicity, yielding the largest interaction

Figure 6. The equilibrium configurations of (a) deprotonated aspartic acid analogue MeCOO$^-$, (b) protonated lysine analogue MeNH$_3^+$, (c) protonated arginine analogue MeGuaH$^+$ complexes in solvent. The bond distances are in Å.

strength of 1.70 eV among the AAs. The dispersion contribution to the binding energy, on the other hand, can be correlated with the polarizability of analogue molecules (figure S4, supplementary information). The three AAs, MePh, MePhOH and MeInd have the largest polarizability values of 88.44, 94.65 and 128.23 Bohr^3, respectively, thereby the largest contributions from the dispersion terms to the binding energy of the complexes (figure 4).

3.3. Charged AAs

The pH condition of an aqueous solution could affect the form of the acidic and basic amino acids, modifying them from neutral to charged species. The equilibrium constant pK_a for the side chains of aspartic acid, lysine and arginine are 3.65, 10.53 and 12.48, respectively [38]. Therefore, under neutral pH conditions (i.e. pH = 7), the acidic amino acids take the deprotonated form, while the basic amino acids take the protonated form. Figure S5 of the supplementary information displays the equilibrium configurations of some of the charged AAs, including the deprotonated aspartic acid analogue MeCOO$^-$; the protonated lysine analogue MeNH$_3^+$ and the protonated arginine analogue MeGuaH$^+$.

Table 3 lists the calculated binding energy of the charged analogue molecules interacting with silicene and figure 6 displays their equilibrium configurations in solvent, indicating the results to be different from those obtained for the neutral analogues. For the acidic analogue MeCOOH, the deprotonated molecule strongly interacts with silicene due to the presence of two unsaturated C=O bonds together with the preference of forming Si–O bonds in the complexes. For the basic analogues MeNH$_2$ and MeGua, however, the protonation of N makes the molecules inactive, yielding significantly smaller binding energy values (see the change in binding energies ΔE_b in table 3). These results are in contrast to the previously reported results [25] on the BN monolayer where it was found that the binding strength of arginine and aspartic acid with

the BN monolayer barely changes, irrespective of the charged state of the amino acids in solvent. However, a variation in the binding energy with the charged states was suggested for the (5,0) BNNT owing to the change in the curvature of the tubular configuration [25]. We attribute the same to the uniquely buckled structure of silicene predicted in this investigation.

4. Summary

Adsorption of AAs on silicene in the gas and solvated phases was investigated using the DFT with vdW correction terms and the implicit solvation model. For canonical analogues, the calculated results suggest that these molecules can be classified into three categories based on the nature of their interactions with silicene. Firstly, the physisorbed configurations, which are weakly bonded by the vdW interactions between the molecules and silicene, include the non-polar molecule MeCH$_3$ and the slightly polar molecule MeSH. Secondly, the chemisorbed configurations involving the Si–O or Si–N bonds show a large variation in interaction strength depending upon the functional group. Silicene is acidic. It interacts stronger with the functional groups with a large basicity with an increasing order of COOH < OH < CONH$_2$ ~ CONHCH$_3$ < NH$_2$ < imidazole < guanidine. Thirdly, the physisorbed configurations stabilized predominantly by the π–π interaction between the phenyl (aromatic) group and silicene.

In solvent, the binding of charged (deprotonated or protonated) analogue molecules to silicene is distinctly different from that of the canonical analogues. For the deprotonated acidic species $-$COO$^-$, the binding increases largely, while for the protonated basic species $-$NH$_3^+$, the binding becomes rather weak.

Overall, the results show that the amino acid lateral chains that are intrinsically more prone to strongly interact with the monolayer are likely to dominate the interface between protein and silicene under physiological conditions.

Acknowledgments

References

[1] Vogt P, De Padova P, Quaresima C, Avila J, Frantzeskakis E, Asensio M C, Resta A, Ealet B and Le Lay G 2012 Silicene: compelling experimental evidence for graphene like two-dimensional silicon *Phys. Rev. Lett.* **108** 155501

[2] Lin X and Ni J 2012 Much stronger binding of metal adatoms to silicene than to graphene: a first-principles study *Phys. Rev. B* **86** 075440

[3] Sivek J, Sahin H, Partoens B and Peeters F M 2013 Adsorption and absorption of boron, nitrogen, aluminum, and phosphorus on silicene: stability and electronic and phonon properties *Phys. Rev. B* **87** 085444

[4] Sahin H and Peeters F M 2013 Adsorption of alkali, alkaline-earth, and 3d transition metal atoms on silicene *Phys. Rev. B* **87** 085423

[5] Tritsaris G A, Kaxiras E, Meng S and Wang E 2013 Adsorption and diffusion of lithium on layered silicon for li-ion storage *Nano Lett.* **13** 2258–63

[6] Wang J, Li J, Li S-S and Liu Y 2013 Hydrogen storage by metalized silicene and silicane *J. Appl. Phys.* **114** 124309

[7] Huang B, Xiang H J and Wei S-H 2013 Chemical functionalization of silicene: spontaneous structural transition and exotic electronic properties *Phys. Rev. Lett.* **111** 145502

[8] Feng J-W, Liu Y-J, Wang H-X, Zhao J-X, Cai Q-H and Wang X-Z 2014 Gas adsorption on silicene: a theoretical study *Comput. Mater. Sci.* **87** 218

[9] Hu W, Xia N, Wu X, Li Z and Yang J 2014 Silicene as a highly sensitive molecule sensor for NH_3, NO and NO_2 *Phys. Chem. Chem. Phys.* **16** 6957

[10] Prasongkit J, Amorim R G, Chakraborty S, Ahuja R, Scheicher R H and Amornkitbamrung V 2015 Highly sensitive and selective gas detection based on silicene *J. Phys. Chem. C* **119** 16934–40

[11] Garc´ıa G, Atilhan M and Aparicio S 2015 Adsorption of choline benzoate ionic liquid on graphene, silicene, germanene and boron-nitride nanosheets: a DFT perspective *Phys. Chem. Chem. Phys.* **17** 16315–26

[12] Wang X, Liu H and Tu S T 2015 Study of formaldehyde adsorption on silicene with point defects by DFT method *RSC Adv.* **5** 65255–63

[13] Amorim R G and Scheicher R H 2015 Silicene as a new ultrafast DNA sequencing device *Nanotechnology* **26** 154002

[14] Suman C and Debnarayan J 2016 A theoretical review on electronic, magnetic and optical properties of silicene *Rep. Prog. Phys.* **79** 126501

[15] Chen L, Feng B and Wu K 2013 Observation of a possible superconducting gap in silicene on Ag (1 1 1) surface *Appl. Phys. Lett.* **102** 081602

[16] Feng B, Ding Z, Meng S, Yao Y, He X, Cheng P, Chen L and Wu K 2012 Evidence of silicene in honeycomb structures of silicon on Ag (1 1 1) *Nano Lett.* **12** 3507–11

[17] Mannix J, Kiraly B, Fisher B L, Hersam M C and Guisinger N P 2014 Silicon growth at the two-dimensional limit on Ag (1 1 1) *ACS Nano* **8** 7538–47

[18] Meng L *et al* 2013 Buckled silicene formation on Ir(1 1 1) *Nano Lett.* **13** 685–90

[19] Fleurence A, Friedlein R, Ozaki T, Kawai H, Wang Y and Yamada- Takamura Y 2012 Experimental evidence for epitaxial silicene on diboride thin films *Phys. Rev. Lett.* **108** 245501

[20] Aizawa T, Suehara S and Otani S 2014 Silicene on zirconium carbide (1 1 1) *J. Phys. Chem. C* **118** 23049–57

[21] Lasave L C, Urteaga R, Koropecki R R, Gonzalez V D and Arce R D 2013 Real-time study of protein adsorption kinetics in porous silicon *Colloids Surf. B* **111** 354–9

[22] Rahsepar F R, Moghimi N and Leung K T 2016 Surface-mediated hydrogen bonding of proteinogenic α-amino acids on silicon *Acc. Chem. Res.* **49** 942–51

[23] Razvag Y, Gutkin V and Reches M 2013 Probing the interaction of individual amino acids with inorganic surfaces using atomic force spectroscopy *Langmuir* **29** 10102–9

[24] Rimola A 2015 Intrinsic ladders of affinity for amino-acid-analogues on boron nitride nanomaterials: a B3LYP-D2* periodic study *J. Phys. Chem. C* **119** 17707–17

[25] Waters K, Pandey R and Karna S P 2017 Amino acid analogue-conjugated BN nanomaterials in a solvated phase: first principles study of topology-dependent interactions with a monolayer and a (5,0) nanotube *ACS Omega* **2** 76–83

[26] Becke A D 1993 Density-functional thermochemistry. III. The role of exact exchange *J. Chem. Phys.* **98** 5648

[27] Lee C T, Yang W T and Parr R G 1988 Development of the Colle–Salvetti correlation-energy formula into a functional of the electron density *Phys. Rev. B* **37** 785

[28] Frisch M J *et al* 2009 *Gaussian09, Revision D.01* (Wallingford, CT: Gaussian, Inc.)

[29] Grimme S 2006 Semiempirical GGA-type density functional constructed with a long-range dispersion correction *J. Comput. Chem.* **27** 1789–99

[30] Tomasi J, Mennucci B and Cammi R 2005 Quantum mechanical continuum solvation models *Chem. Rev.* **105** 2999–3093

[31] Weinhold F and Carpenter J E 1988 *The Structure of Small Molecules and Ions* ed R Naaman and Z Vager (New York: Plenum) pp 227–36

[32] Seel M and Bagus P 1981 Adsorption and surface penetration of atomic hydrogen at the open site of Si(1 1 1): an *ab initio* cluster-model study *Phys. Rev. B* **23** 5464–71

[33] Saikia N, Seel M and Pandey R 2016 Stability and electronic properties of 2D nanomaterials conjugated with pyrazinamide chemotherapeutic: a first-principles cluster study *J. Phys. Chem. C* **120** 20323–32

[34] Seel M and Pandey R 2016 Proton and hydrogen transport through two-dimensional monolayers *2D Mater.* **3** 25004

[35] Cahangirov S, Topsakal M, Aktürk E, Şahin H and Ciraci S 2009 Two- and one-dimensional honeycomb structures of silicon and germanium. *Phys. Rev. Lett.* **102** 236804

[36] Wang Z, He H, Slough W, Pandey R and Karna S P 2015 Nature of interaction between semiconducting nanostructures and biomolecules: chalcogenide QDs and BNNT with DNA molecules *J. Phys. Chem. C* **119** 25965–73

[37] Singla P, Riyaz M, Singhal S and Goel N 2016 Theoretical study of adsorption of amino acids on graphene and BN sheet in gas and aqueous phase with empirical DFT dispersion correction *Phys. Chem. Chem. Phys.* **18** 5597

[38] Lide D R 1991 *Handbook of Chemistry and Physics* 72nd edn (Boca Raton, FL: CRC Press)